

2

REPORT DOCUMENTATION PAGE		READ INSTRUCTIONS BEFORE COMPLETING FORM
1. REPORT NUMBER 16810.6-MS	2. GOVT ACCESSION NO. A127410	3. RECIPIENT'S CATALOG NUMBER N/A
4. TITLE (and Subtitle) Double Slip Plane Crack Model	5. TYPE OF REPORT & PERIOD COVERED Reprint	
	6. PERFORMING ORG. REPORT NUMBER N/A	
7. AUTHOR(s) J. Veertman I.-H. Lin R. Thomson	8. CONTRACT OR GRANT NUMBER(s) DAAG ARO 36-82	
	9. PERFORMING ORGANIZATION NAME AND ADDRESS National Bureau of Standards Boulder, CO 80303	
11. CONTROLLING OFFICE NAME AND ADDRESS U. S. Army Research Office F. O. Box 12011 Research Triangle Park, NC 27709	10. PROGRAM ELEMENT, PROJECT, TASK AREA & WORK UNIT NUMBERS N/A	
	12. REPORT DATE 1983	
14. MONITORING AGENCY NAME & ADDRESS (if different from Controlling Office)	13. NUMBER OF PAGES 10	
	15. SECURITY CLASS. (of this report) Unclassified	
	15a. DECLASSIFICATION/DOWNGRADING SCHEDULE	
16. DISTRIBUTION STATEMENT (of this Report) Submitted for announcement only.		
17. DISTRIBUTION STATEMENT (of the abstract entered in Block 20, if different from Report) B		
18. SUPPLEMENTARY NOTES		
19. KEY WORDS (Continue on reverse side if necessary and identify by block number)		
20. ABSTRACT (Continue on reverse side if necessary and identify by block number)		

DTIC
ELECTE
APR 21 1983

83 04 21 034

DOUBLE SLIP PLANE CRACK MODEL

J. WEERTMAN¹, I.-H. LIN² and R. THOMSON^{3*}

¹Department of Materials Science and Engineering, and Materials Research Center,
Northwestern University, Evanston, IL 60201, U.S.A.

²Fracture and Deformation Division National Bureau of Standards, Boulder, CO 80303, U.S.A.

³Center for Materials Science, National Bureau of Standards, Washington, DC 20234, U.S.A.

(Received 12 April 1982; in revised form 22 October 1982)

Abstract—In this paper a simple crack model is proposed and the behavior of this crack under stress is explored. The crack consists of an ordinary Griffith crack, but on either side of this crack, at a distance w , exist two slip planes that are parallel to the crack plane. It is assumed that slip can only take place on these two planes. Elsewhere the material is elastic. When w is set equal to zero the crack becomes a Bilby-Cottrell-Swinden crack. This crack model simulates in a simple way the elastic crack tip enclave model of a crack. Because w has a finite value the material around the crack tip is elastic. The crack is considered to be stressed in either mode II (plane strain shear) or mode III (anti-plane strain shear). It is found that for a virgin, stationary crack the stress intensity factor at the crack tip is equal to the conventional stress intensity factor when the stress is raised under a monotonically increasing load. However, when the crack tip advances under such a load the crack tip stress intensity factor is smaller than the conventional stress intensity factor. The fracture stress is proportional to the surface energy of the solid raised to a power. In general, this power is not equal to one half. For cyclic loading by using qualitative arguments it is shown that the crack can grow an incremental distance each cycle, and the growth law is a fourth power Paris equation.

Résumé—Dans cet article, nous proposons un modèle simple pour une fissure dont nous étudions le comportement sous contrainte. Cette fissure est une fissure ordinaire de Griffith, mais il existe de chaque côté de la fissure, à une distance w , deux plans de glissement parallèles au plan de la fissure. Nous supposons que le glissement ne peut se produire que sur ces deux plans. Partout ailleurs, le matériau est élastique. Lorsque w égale zéro, la fissure devient une fissure de Bilby, Cottrell et Swinden. Ce modèle de fissure permet de simuler simplement le modèle d'enclave d'une extrémité de fissure élastique. w ayant une valeur finie, le matériau autour de l'extrémité de la fissure est élastique. Nous considérons que la fissure est mise sous contrainte selon le mode II (cisaillement plan) ou le mode III (cisaillement anti-plan). Dans le cas d'une fissure vierge stationnaire, le facteur d'intensité de la contrainte à l'extrémité de la fissure est égal au facteur d'intensité de contrainte classique lorsque l'on augmente la contrainte de manière monotone. Cependant, lorsque l'extrémité de la fissure avance sous l'effet d'une telle contrainte, le facteur d'intensité de la contrainte à l'extrémité de la fissure est plus petit que le facteur d'intensité de contrainte classique. La contrainte de rupture est proportionnelle à une puissance de l'énergie superficielle du solide: en général, cette puissance n'est pas égale à un demi. Dans le cas d'une charge cyclique, des arguments qualitatifs montrent que la fissure peut se propager sur une distance qui augmente à chaque cycle, et que la loi de croissance est une équation de Paris de degré quatre.

Zusammenfassung—Ein einfaches Rißmodell wird vorgeschlagen. Insbesondere wird das Verhalten des Risses unter einer angelegten Spannung untersucht. Der Riß ist ein gewöhnlicher Griffith-Riß. Auf beiden Seiten dieses Risses jedoch finden sich zwei Gleitebenen parallel zur Rißebene im Abstand w . Es wird angenommen, daß Gleitung nur auf diesen beiden Ebenen abläuft, ansonsten ist das Material elastisch. Mit $w = 0$ erhält man einen Riß entsprechend Bilby-Cottrell-Swinden. Das vorgelegte Modell beschreibt auf einfache Weise das Enklavenmodell einer elastischen Rißspitze. Da w einen endlichen Wert besitzt, ist die Rißspitze elastisch. Es wird angenommen, daß der Riß entweder in Mode II (ebene Scherung) oder Mode III (anti-ebene Scherung) Spannungsmäßig belastet wird. Bei einem frischen stationären Riß gleicht der Spannungsintensitätsfaktor an der Rißspitze dem konventionellen Spannungsintensitätsfaktor, wenn die Spannung mit einer monoton ansteigenden Last erhöht wird. Wenn sich jedoch die Rißspitze unter einer solchen Last ausbreitet, dann wird der Spannungsintensitätsfaktor kleiner als der konventionelle. Die Bruchspannung ist proportional zur Oberflächenenergie des Festkörpers hoch einer Potenz, die nicht ein halb ist. Qualitative Argumente zeigen, daß der Riß unter zyklischer Belastung bei jedem Zyklus ein wenig wachsen kann; das Wachstum wird durch eine Parisgleichung der vierten Potenz beschrieben.

INTRODUCTION

In this paper a very simple crack model is considered in order to elicit the fundamental features of a crack interacting with a deformation field generated by the

stress concentration at the crack tip, and to confirm results of an earlier more complex elastic enclave model [1, 2]. In our model, we assume that slip can occur on two slip planes, parallel to the cleavage plane, but displaced from it by distance w in each direction, Figs 1 and 2. Our work will be couched in

*Supported in part by U.S. Army Research Office.

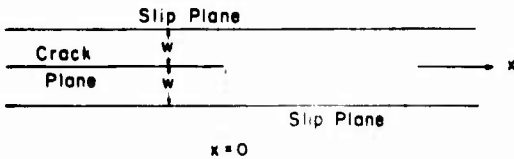


Fig. 1. Double slip plane model. The crack is assumed to be an atomically sharp slip crack on the negative x -axis with the tip at the origin. Two planes parallel to the crack plane are permitted for dislocation generation and slip. The planes are assumed to be a distance w from the crack plane. Mode III or II will be assumed throughout for purposes of analysis.

terms of the shielding afforded a crack by the deformation field generated by the stress concentration at the crack tip.

For our simple model, we will show that (1) the initial response of a crack to the generation of a deformation field on the two slip planes is essentially nonshielding in character; (2) that as the crack propagates, the stress intensity at the crack tip, K_i , is shielded from the external stress intensity, K , that is $K > K_i$; and (3) that cyclic loading with work hardening can lead to crack growth.

These results are based upon a particular form of one dimensional slip, and we can expect the results will be modified if slip occurs on planes which intersect the cleavage plane. We will discuss these modifications in a qualitative way, but the simple model nevertheless leads to results which highlight how the behavior of materials with real dislocations will differ from that of a plastic continuum. We also note here that our one dimensional model has certain similarities to the early BCS model [3] of fracture, but the main physical picture resulting in our case is different in important ways from the BCS results. We will work in mode III and mode II because the mathematics will be accessible to an analytic approach (especially in mode III), but the general features are expected to apply to the more important mode I, as well. Finally, we note that our paper addresses the behavior of a crack whose tip is atomically sharp.

THE CRACK TIP STRESS INTENSITY FACTOR

In an earlier paper [4], by one of us, we showed for a set of dislocations in mode III surrounding a sharp crack, that

$$\bar{G} = \bar{g}_i + \sum_d \bar{g}_d = \frac{K^2}{2\mu} \quad (1)$$

where \bar{g} is the force per unit length exerted on the defect, here referred to as i for the crack, d for a dislocation, and \bar{G} is the force on the conglomerate composed of crack plus dislocation distribution. G and g are complex functions of $x + iy$, the crack is supposed to lie along the negative x -axis with the tip at the origin, the real part of \bar{g} or \bar{G} is the x -component of the force, and the imaginary part the

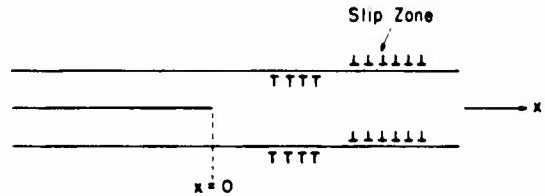


Fig. 2. Double slip plane model. Dislocations are distributed symmetrically on the two planes.

y -component. \bar{g} is the complex conjugate of g , μ is the shear modulus. The physical interpretation of equation (1) is that the total force $\bar{G} = K^2/2\mu$ in terms of the far field external stress intensity factor (small scale yielding) is linearly composed of the separate forces on crack and dislocations. Equation (1) is valid only when the dislocation distribution is symmetric (the situation considered in this paper) about the x -axis. The local force on the crack by itself is given by

$$\begin{aligned} \bar{g}_i &= K_i^2/2\mu \\ K_i &= K - K_d \\ K_d &= \frac{1}{2} \sum_j \mu b_j \left(-\frac{1}{\sqrt{2\pi\zeta_j}} + \frac{1}{\sqrt{2\pi\bar{\zeta}_j}} \right) \end{aligned} \quad (2)$$

ζ_j is the position of the j th dislocation in the complex plane. K_d is the screening contribution to K at the crack tip due to the dislocation distribution. The physical meaning of equation (2) is that the crack is either screened (or antiscreened) from the externally imposed stress represented by the external K -field, depending on the sign of b_j .

In Fig. 2, since the x -component of force on a dislocation is given by $\text{Re}(\bar{g}_d) = \tau b_j$, where τ is the shear stress on the slip plane, we can also write

$$\bar{g}_i + \sum_j \tau_j b_j = \bar{g}_i + 2 \int \tau(x) B(x) dx = K^2/2\mu. \quad (3)$$

Here we have replaced the discrete dislocations by a continuous linear distribution $db_j = B(x)dx$. The in-

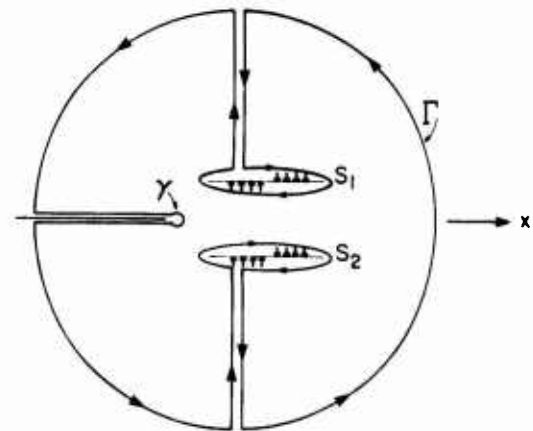


Fig. 3. Path for J -integral. Γ is a path outside the crack and all dislocations. γ encloses the crack tip, and S_1 and S_2 enclose the two symmetric dislocation distributions on the parallel slip planes.

tegration is carried out on only one slip plane, but in Fig. (2), we assume that the distribution on each slip plane is identical, accounting for the factor 2 before the integration in equation (3).

Equation (3) is easily generalized to mode II and mode I by taking the J -integral (the J -integral of Rice [5] which is identical in the elastic case to the F_I integral proposed earlier by Eshelby [6]) path shown in Fig. 3. (This is in fact what was done in Ref. [4].) The external path enclosing crack and dislocations yields the total crack extension force, $G = K^2/2 \mathcal{K} \mu$, where \mathcal{K} is a mode dependent factor given below, g_i is $K_i^2/2 \mathcal{K} \mu$, and the path around the dislocation distribution is given by

$$\text{Re}(G) = \int_{\Gamma_1 + \Gamma_2 + \Gamma_3 + \Gamma_4} \left(W' dy - \tau \frac{\partial u}{\partial x} dx \right). \quad (4)$$

Thus we can replace (3) by the more general

$$\bar{g}_i + 2 \int_{-\infty}^{\infty} \tau(x) B(x) dx = K^2/2 \mathcal{K} \mu \quad (5)$$

$$\mathcal{K} = \begin{cases} 1 & \text{Mode III} \\ 1 - \nu & \text{Mode II.} \end{cases}$$

It should be noted in equation (3) and (5) that we are considering only the case when a continuous dislocation distribution $B(x)$ does not have a stress singularity associated with it. This is the case when $\tau(x)$ is finite everywhere on the slip planes. If stress singularities exist at an end of a dislocation distribution, as they would if dislocations were piled up against an obstacle, the integrals of (3) and (5) must be evaluated with great care. For example, in that case, a finite contribution is made to the J -integral from the tips of the distribution, whereas when $\tau(x)$ is everywhere finite, the contribution from the tips is zero [7].

It should be noted that equation (2) and (5) can be rewritten in terms of the (total) dislocation produced shielding or antishielding stress intensity factor, L , of Rice and Thomson [8]. Equation (2) then becomes

$$K_i = K + L \quad (6)$$

where L has a positive value in the antishielding case and a negative value in the shielding situation. In equation (5) let the integral term be set equal to

$$\int_{-\infty}^{\infty} \tau(x) B(x) dx = \frac{\mathcal{K}}{4\mu} I \quad (7)$$

where I is defined by this equation. Equation (5) can be written as

$$K_i = K(1 - I/K^2)^{1/2}. \quad (8)$$

Combining equations (6) and (8) gives

$$L = -K + (K^2 - I)^{1/2}. \quad (9)$$

STATIONARY CRACK

We now explore the result of a sequence of events in which we allow a sharp slip crack to generate a

dislocation distribution on the discrete slip planes of Figs 1 and 2, but require the crack to remain stationary. Specifically, (1) we place a slit crack in an otherwise perfect elastic medium; (2) we allow sources to operate anywhere on each of the two slip planes so that identical distributions are produced on each. It is a property of these distributions that equal numbers of dislocations of positive and negative burgers vector are produced on each slip plane because a dislocation source always produces dislocations in pairs. Thus

$$\int_{-\infty}^{\infty} B(x) dx = 0;$$

(3) we allow the dislocation distribution to come into force equilibrium, so that the total force acting on a dislocation is zero. The elastic portion of the force will be made up of the total elastic shear stress, τ , acting at the dislocation in question from all the other dislocations and the stress from the crack. There will also be a force due to lattice friction, due to the effective lattice friction stress which we call σ_f . Thus we can write in equilibrium that

$$\tau(x_i) = -\sigma_f(x_i). \quad (10)$$

If σ_f is a simple constant, then the crack model would simulate a perfectly plastic solid. If σ_f increases with the displacement, D , across a slip plane where

$$D(x) = \int_{-\infty}^x B(x) dx \quad (11)$$

then the crack model would simulate work hardening. (The reader will note that true "work hardening" is not really consistent with our model, because the interaction with the other dislocations is presumably included in equation (3) or (5). In true work hardening, "redundant" dislocations of opposite sign are all important. The net Burgers vector of these redundant dislocations in any small volume element is equal to zero, and consequently they do

not appear in a dislocation distribution function $B(x)$. We therefore have to assume for this purpose that there are other effects which increase σ_f , perhaps lattice debris, other dislocations in walls, etc., which we do not otherwise explicitly countenance. (However, making σ_f depend upon D does give us an analytic way to bring the real effects of deformation into our simplified model.)

We now calculate the total elastic force on the dislocations from equation (3) or (5). This is given by

$$\sum \bar{g}_d = 2 \int_{-\infty}^{\infty} \tau(x) B(x) dx = -2 \int_{-\infty}^{\infty} \sigma_f B(x) dx. \quad (12)$$

In the spirit of the last paragraph, we now assume that $\sigma_f = \sigma_f(D)$. Since $B(x) dx = dD$, we then have

$$\int_{-\infty}^{\infty} \sigma_f(x) B(x) dx = \int_{D=0}^{D=0} \sigma_f(D) dD = 0. \quad (13)$$

Likewise, I given in equation (7) is zero. Substituting for $\Sigma \bar{g}_d$ in (3) or (5), we then have

$$\bar{g}_t = \frac{K_t^2}{2\mathcal{H}'\mu} = \frac{K^2}{2\mathcal{H}'\mu} \quad (14)$$

(or from equations (8) and (9) $K_t = K$ and $L = 0$), and the crack tip is not screened by the deformation zone. Although this result is derived for two parallel slip planes, it is also valid for an arbitrary number of slip planes parallel to the cleavage plane in which symmetry about the x axis is preserved.

This result is so striking that it deserves additional discussion and verification. (This result, as pointed out by a reviewer, is obvious from the original interpretation of Eshelby's [6] F_1 integral. F_1 measures the resultant on the crack tip of the forces due to the elastic field on all the dislocations, which is opposite to the traction stress. With equal numbers of dislocations of opposite sign, and each opposed by the traction stress, only the crack extension force remains.) Suppose we have only one pair of dislocations of opposite sign on each of the slip planes of Fig. 4, and assume mode III. Then we explore the possibility of setting the dislocation contribution to K equal to zero

$$\begin{aligned} 0 &= K_d = \mu b \operatorname{Re} \left(\frac{1}{\sqrt{2\pi\zeta_1}} - \frac{1}{\sqrt{2\pi\zeta_2}} \right) \\ &= \frac{\mu b}{\sqrt{2\pi w}} \left(\cos \frac{\theta_1}{2} \sqrt{\sin \theta_1} - \cos \frac{\theta_2}{2} \sqrt{\sin \theta_2} \right). \end{aligned} \quad (15)$$

For any value of θ_1 (where we place b_1) in the range $0 < \theta_1 < \pi$, there is another and different value for θ_2 (where we place b_2) for which $K_d = 0$ (except for the single angle where only one value of θ satisfies (15), $\theta = 2 \tan^{-1} 1/\sqrt{3}$). From equations (3) and (4) when $K_d = 0$

$$\operatorname{Re}(\bar{g}_1 + \bar{g}_2) = 0. \quad (16)$$

and if there exists an effective lattice friction stress, σ_f , which is the same for each dislocation, since $b_1 = -b_2$, we have constructed an equilibrium configuration for which there is no screening. Equation (14) is thus confirmed. We note that as $w \rightarrow 0$ in equation (15) the argument degenerates.

The nonshielding result of equation (14) is a special case for slip planes which are parallel to the cleavage plane. However, even in cases where this geometry is not approximately a valid picture, we retain some features of the nonshielding result. The reason is that

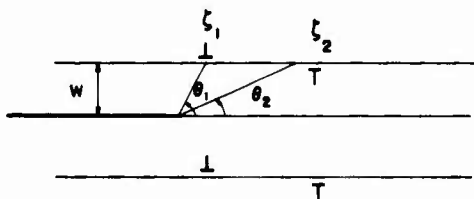


Fig. 4. Schematic figure for two pairs of dislocations in non-shielding configuration. Coordinates of dislocations are labelled.

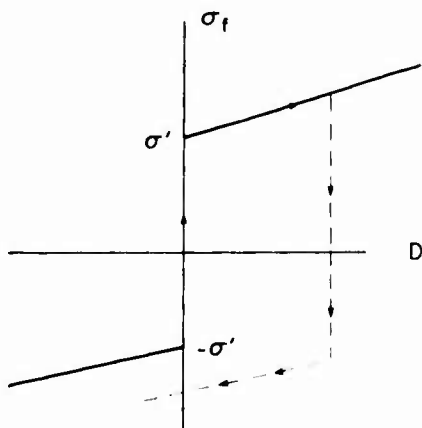


Fig. 5. Friction law. Dashed lines show the law obeyed for reversed slip following forward slip with work hardening. The full line for negative slip indicates a fully reversible slip law.

in all cases, dislocations will initially be formed in pairs, and the pair dipoles will be so oriented that the antishielding dislocation will be closest to the crack, and will be attracted toward it. Hence, the initial effect of loading a stationary crack will not be to shield it, but shielding can only occur as a later stage of the total process. We turn now to a discussion of possible later stages.

GROWING CRACK

Let us suppose we have a stationary crack with two active double slip planes as described in the previous section in which $K_d = 0$ and $K = K_t$, and that we begin to increase K in adiabatic fashion. When the value of K_t reaches the Griffith critical value for crack propagation in a perfectly brittle solid, the crack propagates. However, when this happens, the relations between the elastic stresses, τ and σ_f which are responsible for establishing the equilibrium of the dislocation configuration become altered, and the nonshielding solution, equation (10), breaks up. In effect, the antishielding dislocations undergo reversed slip if they are carried along with the propagating crack, and σ_f for these dislocations then changes sign. See Fig. (5). This reversal of σ_f means that the crack will leave the antishielding component behind, and the shielding dislocations will be pushed ahead of it. The net effect is that only the shielding dislocations are left in the distribution. The sum in equation (3) to obtain K_d is then finite and positive, and $K > K_t$, so that the crack tip is shielded.

That antishielding dislocations cannot be carried along by a growing crack can be understood from the following considerations. If antishielding dislocations were carried along and thus move in the same direction as the shielding dislocations, the stress on the slip plane must change discontinuously from the value σ_f to the value $-\sigma_f$ if there is no gap on the slip plane between the shielding and the antishielding

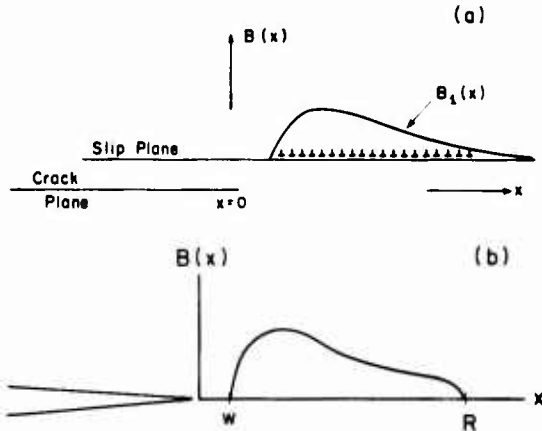


Fig. 6. Dislocation distribution. (a) Schematic dislocations for one of a pair of parallel slip planes. The distribution near $x = w$ falls to zero smoothly. (b) For the purposes of analyses, we assume the dislocation distribution is on the crack plane, and that the closest approach of the dislocation distribution to the crack tip is w .

dislocations. But a stress discontinuity of this type can be produced only by a logarithmically divergent dislocation distribution which has the same sign on either side of the discontinuity. (This can be shown using the usual Hilbert transform integral equations that appear in, for example, the BCS crack theory.) Hence no solution exists if no gap exists. But suppose a gap does exist. The antishielding dislocation must trail after the shielding dislocations. If they were in the forward position they would be pulled into the shielding dislocations because of the attractive stress fields of both the crack tip and the shielding dislocations. Because the friction stress is supposed to have a reversed sign in the region of the antishielding dislocations, the dislocations, too, according to equation (3) or (7), are shielding dislocations and cause a reduction in the value of K_I . But the antishielding stress intensity factor L of the antishielding dislocations cannot change their sign according to the equations of Rice and Thomson [5]. Thus our supposition that there is a zone of antishielding dislocations, with a reversed friction stress that is carried along with the crack tip through the attraction of these dislocations towards the shielding dislocations, has led to an inconsistent result and the assumption must be incorrect.

We will now carry out an analysis of the shielding to show how it depends in detail on the material parameters. We shall assume the distance, w , is small compared to the length over which the dislocations are distributed. In this case, the closest approach of any dislocation to the crack tip will be w . Further, except for those dislocations closest to the tip, the angular part of the crack is negligible, and θ can be taken $\theta = 0$ to good approximation. Thus we can approximate the entire distribution and its effect on the crack by replacing the pair of slip planes with a single line of dislocations on the cleavage plane, but where the distribution begins at $x = w$. That is, we

assume a "dislocation free zone" in front of the crack, to correspond to the slip plane separation, w . See Fig. 6a, b. This strategem allows us to carry out a rigorous analysis.

From Ref. (4) the force on an arbitrary dislocation on the slip line is

$$g_d = \frac{Kh}{\sqrt{2\pi x}} - \frac{\mu b^2}{4\pi x} + \sum_b \frac{\mu b' b}{2\pi} \sqrt{\frac{x'}{x(x-x')}} \quad (17)$$

x is the distance on the cleavage plane from the crack tip to the dislocation, and a sum is taken over all other dislocations at x' of Burgers vector b' . Adopting a continuum limit, we set $db = B(x) dx$, and write

$$\frac{1}{B} \frac{dg}{dx} = \frac{K}{\sqrt{2\pi x}} - \frac{\mu B(x) dx}{4\pi x} + \frac{\mu}{2\pi} \int_w^R \sqrt{\frac{x'}{x(x-x')}} B(x') dx = -\sigma_f(x) \quad (18)$$

$\sigma_f(x)$ on the right is the lattice friction stress, and with it (18) is the condition for equilibrium to be satisfied. We shall take σ_f as a constant in the following, because otherwise the mathematics becomes intractable. The second term is of lower order than the others, and must be dropped. We note that this dropout of the self-image term demonstrates a physical difference between continuum theories and discrete theories. The self-image term is known to be dominant at distances of order b from the crack tip, and thus all continuum theories, because they lose this scale parameter, are essentially helpless to discuss atomic phenomena at the crack tip. Equation (18) can be put in the canonical integral equation form

$$P(x) = \int_w^R \frac{\beta dx'}{x-x'} \\ P(x) = \frac{-2\pi\sqrt{x}}{\mu} \left(\sigma_f + \frac{K}{\sqrt{2\pi x}} \right) \\ \beta(x') = \sqrt{x'} B(x'). \quad (19)$$

This is the standard singular integral discussed by Muskhelishvili [9] and we refer the reader to the paper of Head and Louat [10] for its solution. This problem has been solved recently in a different way by Chang and Ohr [11]. After carrying out the analysis described below, we discovered that Majumdar and Burns [12] in a paper shortly to be published have carried out the solution by a technique very close to our own. However, since we are interested in the analytic results which can be obtained on the assumption that $w \ll R$, we shall indicate our steps in summary form below.

The uniqueness relation of Head and Louat [10] for a distribution $B(x)$ which has zero values at w and R

is given by

$$\begin{aligned} K &= -\sqrt{2\pi} \sigma_f I_1 I_2 \\ I_1 &= \int_w^R \frac{\sqrt{x'}}{\sqrt{(x'-w)(R-x')}} dx' \simeq \sqrt{2R} \\ &\quad + \frac{w}{2\sqrt{R}} \ln 4R/w \\ I_2 &= \int_w^R \frac{dx'}{\sqrt{(x'-w)(R-x')}} = \pi. \end{aligned} \quad (20)$$

The integral equation is inverted by the equation

$$\begin{aligned} B(x) &= -\frac{2}{\pi\mu} \sqrt{\frac{(x-w)(R-x)}{x}} \left\{ \frac{KI_3(x)}{\sqrt{2\pi}} + \sigma_f I_4 \right\} \\ I_3 &= \int_w^R \frac{1}{\sqrt{(x'-w)(R-x')}} \frac{dx'}{x-x'} \equiv 0 \\ I_4 &= \int_w^R \frac{\sqrt{x'}}{\sqrt{(x'-w)(R-x')}} \frac{dx'}{x-x'}. \end{aligned} \quad (21)$$

Using the uniqueness relation, (20), and carrying out the integration to find K_f from (3), we have

$$K_f = K - \frac{\mu}{\sqrt{2\pi}} \int_w^R \frac{B(x) dx}{\sqrt{x}}. \quad (22)$$

Combining the previous equations we find

$$\frac{K_f}{K} = 1 + \frac{1}{\pi^2} \frac{I_1}{I_2} \int_w^R \frac{\sqrt{(x-w)(R-w)}}{\sqrt{x}} \frac{I_4(x)}{x} dx. \quad (23)$$

We carry out the integrations indicated in the limit $R \gg w$ by elementary integrals and find to lowest order in w/R

$$\begin{aligned} \frac{K_f}{K} &= \frac{3}{2\pi} \sqrt{\frac{w}{R}} (\ln 4R/w + 4/3) \\ K_f &= \frac{-3\sqrt{2}}{\pi^{3/2}} \sigma_f \sqrt{w} \times (\ln 4R/w + 4/3). \end{aligned} \quad (24)$$

This result is equivalent to that obtained by Majumdar and Burns [12]. Its form in equation (24) is particularly useful to us because of its simple analytic character.

It should be noted that the result given by equation (24) says that the total integrated burgers vector of the dislocations ahead of the crack tip is the maximum possible subject to the condition that at a distance w ahead of the crack tip the stress is equal to σ_f . It is, of course, possible to find a solution in which a smaller number of dislocations are present ahead of the crack tip. The value of K_f then is larger than that given by equation (24). But in this situation the stress would be larger than σ_f at the distance w . If more dislocations were present, the dislocation distribution would either have to start at a distance smaller than w , or if the dislocations were restricted to start at w , an infinite stress at this position is required to prevent the dislocations from approaching closer to the crack tip.

We note that equation (24) contains the shielding physics which the BCS model does not. For example, if we let $w \rightarrow 0$ as in the BCS model, $K_f \rightarrow 0$, wherein we lose the K field of the underlying crack entirely. For us, w will retain the meaning of the separation between slip planes. We note that for slip planes actually separated from the cleavage plane, that is, as shown in Fig. 1 rather than Fig. 6b, the solution very near the tip will be somewhat different from the cleavage plane model of equation (23). The distribution near the crack tip will not cut off as sharply as in (21), but this difference is expected to be a minor quantitative effect rather than a qualitative one.

To incorporate work hardening directly into the dislocation equilibrium equations, (18), σ_f would have to be a function of the local density $B(x)$, and there would be no analytic solution of the integral equation. However, if we allow σ_f to be a function of the total dislocation content of the slip plane, we can then incorporate a simple work hardening law into our results. Thus, we shall set

$$\begin{aligned} \sigma_f &= \sigma_0 (D^* D_0)^m \\ D^* &= \int_w^R B(x) dx \end{aligned} \quad (25)$$

σ_0 and D_0 are constants, and m is the work hardening exponent, $0 < m < 1$.

To the lowest order in w/R , for mode III, we integrate $B(x)$ to obtain

$$D^* = \frac{2K}{\mu} \sqrt{\frac{R}{2\pi}}. \quad (26)$$

Then, combining equation (24), (25) and (26) we obtain

$$\begin{aligned} K &= \left(\frac{K_f}{w} \right)^{(1+m)/4m} \beta \\ \beta &= \left(\frac{\pi^3}{18} \right)^{(1+m)/4m} \\ &\quad \times \frac{\sqrt{2D_0\mu}}{\sigma_0^{1/2m} (\ln 4R/w + 4/3)^{(1+m)/2m}}. \end{aligned} \quad (27)$$

From equation (27) and our previous discussion, we can now predict the overall behavior of a bare crack when at time $t = 0$, we load it up and allow deformation to proceed in the vicinity of the crack tip. We must first assume that the crack will propagate whenever K_f exceeds a critical value for cleavage of a pure brittle crack in the solid, K_{Ic} . In an uncomplicated situation, we must reasonably assume this critical value is the Griffith value

$$K_{Ic} = \sqrt{4\gamma\mu/\mathcal{K}} \quad (28)$$

where γ is the intrinsic surface energy of the solid. At time $t = 0$, the crack is loaded, and dislocation pairs are created on the slip planes. For a short transient period, the pairs remain in the vicinity of the crack

tip, and the K_i remains near zero. The external K is transmitted directly to the crack tip unshielded. The crack will accelerate as soon as K_{ch} is achieved, the shielding dislocations will be shoved ahead of the crack, and antishielding ones will be sloughed off at the rear. As the shielding "charge" is built up around the tip with the loss of the antishielding dislocations, the crack will require larger and larger external K to keep K_i above its critical cleavage value. Ultimately, a steady state is conceivable in which the shielding charge is constant, and in this case, the relation interconnecting the external K , K_{ch} , w , m , etc., will be given by equation (27). Equation (27) then becomes a model fracture criterion for the material.

Equation (27) may be compared with the elastic enclave models of references [1] and [2]. (We have shown separately [13] that the versions of the previous elastic enclave models are equivalent.) Here, however, we have a more satisfying model of cracking in terms of the dislocation theorist. Our model, we believe, should have the same kind of appeal which the original BCS model did, and through it we are able to see intuitively into the role dislocations and their discrete sources play in fracture. We can summarize this section by bringing together the various relations derived which interconnect K , K_i , σ_i , m

$$\frac{K_i}{K} = \frac{3}{2\pi} \sqrt{\frac{w}{R}} (\ln 4R/w + 4/3)$$

$$K = -2\sqrt{2\pi} \sigma_i \sqrt{R}$$

$$\sigma_i = -\sigma_0 (D^*/D_0)^m$$

$$D^* = \frac{K}{\mu} \sqrt{\frac{2R}{\pi}}$$

Our principal result, equation (27), is a particular combination of these equations.

In our model, the sources for the dislocations are assumed to be external to the crack tip, and the parameter, w , is a measure of the inhomogeneity of slip in all real materials. If the crack can itself generate dislocations out of the tip, this process will be governed by an essentially different type of physics which we do not address here.

CYCLIC STRESS

Consider next in a qualitative way "fatigue" growth under an applied cyclic stress. Let the cyclic stress vary from $\sigma = 0$ to $\sigma = \sigma_{\max}$ and the conventional stress intensity factor K vary from $K = 0$ to $K = K_{\max} = \sigma_{\max}(\pi a)^{1/2}$. The fatigue crack will advance an increment each cycle if "work hardening" occurs on the two slip planes, both during forward slip and during reverse slip. To see why, consider Fig. 7. Figure 7a shows schematically a dislocation distribution $B_1(x) = B_{\max}(x)$ that exists when $\sigma = \sigma_{\max}$ and the crack has stopped its advance. This distribution produces a shielding stress intensity factor L_{\max} given by equation (9) to be

$$L_{\max} = -K_{\max} + (K_{\max}^2 - I_{\max})^{1/2} \quad (29)$$

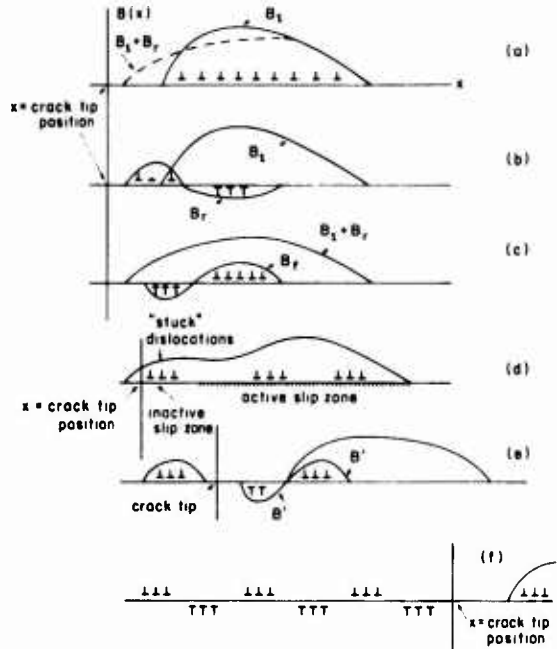


Fig. 7. Cyclic crack advance. Dislocation distribution on one slip plane. (a) At maximum stress (solid line) and when stress is reduced to zero (dashed line). (b) Dislocation distribution of (a) considered as the original distribution and a reversed slip distribution $B_r(x)$. (c) After the stress is again increased to maximum value if the crack tip were not to advance. Forward slip can be considered to occur by creation of additional distribution b_r . (d) Crack advance. Dislocation in inactive slip zone are now "stuck" in slip plane and do not advance. (e) Activation of a slip zone and distribution function B' containing both negative and positive dislocations. The negative dislocation eventually also become stuck. (f) After many stress cycles and many incremental crack advances. A wake of stuck dislocations of alternating sign are left behind.

where I_{\max} is the value of I from (7) when $B(x) = B_{\max}(x)$. Because the crack has stopped but was advancing immediately before the stress reached its maximum value

$$K_i = K_{\max} + L_{\max} = K_{ch} \quad (30)$$

where K_{ch} is given by equation (28) and is the critical stress intensity factor of a Griffith crack. Further crack advance would reduce K_i to a value smaller than K_{ch} , the critical value for brittle propagation of the crack tip. Now let the external stress, σ , and stress intensity factor, K , be reduced to zero. Then, in the absence of the repulsive forces on the dislocations due to the crack K -field, the large dislocation density at the maximum near the crack tip (see Fig. 6a) will be forced in the negative direction on the slip plane (reversed slip) under the mutual repulsions of the dislocations until a new equilibrium distribution is achieved, as shown schematically by the dashed line of Fig. 7a. If the crack tip is locked in position, we expect many of these dislocations to be pushed well behind the crack tip. When they get into this region, however, they are in the presence of the open cleavage plane of the crack. Under these conditions, an inverse

image dislocation distribution is generated across the open crack plane which cancels the long range force fields of these dislocations. In a sense, the crack faces, by converting the whole dislocations into dipoles absorbs these dislocations, so far as their long range stress fields are concerned, almost as effectively as if they were physically absorbed into the open cleavage faces. Only those dislocations which can be sustained by the modified σ_f (see below) under the mutual repulsive interactions from the dislocations will remain in front of the crack.

Secondly, on a microscopic level, we can expect the effect on the crack tip of decreasing K to zero to be important. In the absence of the external stress, σ , because $K_f = L$ from equation (30), K_f is a large negative number, because L is negative. If the crack tip is reversible, it will thus be driven backwards on its cleavage plane. Of course, cracks in materials of even modest ductility should be reversible only in a limited degree, and over very short distances, but if the crack tip can recede, this provides additional room for dislocations to stay ahead of the tip and not get lost behind it. In any case, the negative K_f caused by the dislocation shielding will provide a large closure stress on the crack faces, and if the tip itself remains open, the situation will be analytically complex.

With this general physical picture in mind, we turn to an analysis of our simple model. For definiteness, we assume the crack tip to be locked in position, so far as retrograde motion is concerned. After the external stress is turned off, but before the dislocations are allowed to redistribute, $K_f = L_{\max} < 0$, as noted above. Because of the reversed slip, however, the magnitude of L will be reduced. The reversed slip can be considered to occur by the creation of a new dislocation "reversed" distribution function $B_r(x)$ shown in Fig. 7b, which when added to the distribution $B_{\max}(x)$ gives the dashed distribution of Fig. 7a. Of course, $B_r(x)$ must satisfy $\int B_r(x) dx = 0$. The value of L is given after reversed slip by

$$L = -K_{\max} + (K_{\max}^2 - I_{\max} - I_r)^{1/2} \quad (31)$$

where

$$I = \frac{4\mu}{\pi} \int \tau(x) B(x) dx \quad (32)$$

and $\tau_r(x)$ is the total change of stress that must be produced in the reversed slip zone at point x in order for slip to occur. For the case in which there is no work hardening $\tau_r(x)$ would be equal to $2\sigma_0$, because the stress started out as equal to a constant friction stress, σ_0 , before reversed slip started and the stress has to equal $-\sigma_0$ during the reversed slip. This is the value of $\tau_r(x)$, however, only in those regions of reversed slip where $B_{\max}(x) \neq 0$. Where $B_{\max}(x) = 0$ and reversed slip occurs, $\tau_r(x)$ is smaller than $2\sigma_0$ because the stress on the slip plane was smaller than σ_0 where $B_{\max}(x) = 0$. Thus for the case where no work hardening occurs, τ_r is not a constant over the

integral of equation (32), and I_r is not equal to zero. Because $B_r(x)$ is positive in the regions (see Fig. 7b) where $\tau_r(x)$ is smaller than $2\sigma_0$, the term I_r is a negative quantity. The shielding intensity factor L of equation (31) is a less negative quantity (less shielding) than L_{\max} . This result is also true when work hardening occurs.

Let the stress, which has been reduced to zero, increase again to the level σ_{\max} . Forward slip will occur, as shown in Fig. 7c, in the reversed slip zone. If the crack tip were not to advance the shielding intensity factor L^* is now given by

$$L = -K_{\max} + (K_{\max}^2 - I_{\max} - I_f - I_r)^{1/2} \quad (33)$$

where

$$I_f = \frac{4\mu}{\pi} \int \tau_f(x) B_f(x) dx \quad (34)$$

where $B_f(x)$ is the new additional dislocation distribution produced by the forward slip ($\int B_f(x) dx = 0$) and $\tau_f(x)$ is the total change in stress on the slip plane in the region where $B_f(x) \neq 0$. When no work hardening occurs over the region where $B_{\max}(x) \neq 0$, then $\tau_f(x) = 2\sigma_0$. But where $B_{\max}(x) = 0$, the stress $\tau_r(x)$ will be smaller than $2\sigma_0$ by the identical amount that $\tau_r(x)$ in the same region was smaller than $2\sigma_0$. Because $B_f(x) = -B_r(x)$ when no work hardening occurs, $I_f = -I_r$. Consequently, $L = L_{\max}$ and no crack advance will occur.

Suppose work hardening occurs during slip. Let equation (25) be generalized for reversed slip (see Fig. 5) to give for the friction stress

$$\sigma_f = (\sigma_0/D_0^m)(\sum |D^*|^m) + \sigma' \quad (35)$$

where the sum on D^* is the sum of the absolute values of all displacements that have occurred at any particular point x on a slip plane. (In reversed slip the friction stress is given by equation (35), but with a negative sign on the righthand side of the equation.)

Because of work hardening $B_r(x) \neq -B_f(x)$ and $I_r \neq -I_f$. The increase in the value of $\tau_r(x)$ and $\tau_f(x)$ produced by work hardening can be expected to increase the magnitude of I_r and I_f given by equations (32) and (34). However, the same work hardening will make the magnitude of $B_r(x)$ and $B_f(x)$ smaller, an effect which will decrease the values of I_r and I_f . If the power exponent m of equation (35) is smaller than 1 the effect of work hardening on τ_r and τ_f will be smaller than on B_r and B_f and consequently $|I_r| < I_f$. Thus, if the crack tip were not to advance upon increasing the stress again to $\sigma = \sigma_{\max}$ the shielding intensity factor L is smaller in magnitude than L_{\max} . The crack tip stress intensity factor K_f will be larger than K_{\max} . Thus, the crack tip must advance before σ attains its maximum value. As the crack advances it will leave behind it, "stuck" on the slip plane, part of its dislocation distribution as indicated in Fig. 7d. Part of the distribution is left behind because on the trailing edge of the distribution $|B_r| < B_f$.

As the crack advances and spreads out the distribu-

tion $B_1(x)$ the crack tip stress intensity factor K_I will actually increase further without increasing the stress. Note that I_{\max} is equal to

$$I_{\max} = \frac{4\mu}{\mathcal{K}} \int \tau(x) B_1(x) dx \quad (36)$$

where $\tau(x)$ is equal to the yield stress on the slip plane wherever $B_1(x) \neq 0$. Here $B_1(x)$ is the distribution shown by the solid line of Fig. 7a. Now if the crack advances and spreads out the distribution $B_1(x)$, the trailing "stuck" edge of this distribution will be in regions where the stress on the slip plane is smaller than the yield stress. In the regions where slip is occurring $\tau(x)$ is equal to the yield stress and has the same value as the yield stress in equation (36). Thus the "stretched" dislocation distribution B_{str} of Fig. 7d will lead to a value of I_{str} , with sufficient crack advance, that is smaller than I_{\max} . Therefore, K_I increases in value with crack advance. But this increase cannot go on indefinitely. A large value of K_I means that the stress field of the crack tip is increased. Eventually this increased stress field will produce slip near, but ahead, of the crack tip as shown in Fig. 7e. This slip can be described with still another dislocation distribution function $B'(x)$ where again $\int B'(x) dx = 0$. The positive dislocations of this function are further from the crack tip as shown in Fig. 7e, and move in the direction of the advancing crack tip. The negative dislocations move in the opposite direction. Eventually the negative dislocations in turn will also become stuck on the slip plane, but positive dislocations will join the moving dislocations of the distribution $B_1(x)$. Hence, the total number of positive dislocations increases and the value of I also increases. This increase in turn decreases the value of K_I until once again K_I is equal to K_{ch} . When the applied stress σ has reached the value σ_{\max} , a limited amount of crack growth thus will insure that $K_I = K_{ch}$ and the fatigue crack will stop. In the wake of the fatigue crack (on both of the slip planes) "stuck" dislocations of alternating sign will exist as shown in Fig. 7f.

A rough estimate of the crack growth increment per stress cycle can be made as follows. To have crack advance in each cycle, the crack tip stress intensity factor K_I given by equation (24) must equal K_{ch} during the incremental growth. The work hardening under cyclic slip must, therefore, increase the average value of the friction stress σ_f to the point that $K_I = K_{ch}$. Thus from equation (24) σ_f must attain the value

$$\sigma_f = K_{ch}/\beta \sqrt{w} \quad (37)$$

where β is given by equation (27). Let δa be the increment of crack growth per cycle. From equation (20) when $R \gg w$, the length of a slip zone with an average friction stress σ_f is equal to $\pi K_{\max}^2/8 \sigma_f^2$. The number of cycles n required for the crack to advance this distance is

$$n = \pi K_{\max}^2/8 \sigma_f^2 \delta a. \quad (38)$$

The average displacement D within this slip zone from equation (21) can be shown to be (for one of the slip zones of the two slip planes) equal to $\mathcal{K} K_{\max}^2/6 \sigma_f \mu$. The sum $\Sigma |D|$ thus is of the order of $2nD$ or

$$\Sigma |D| \cong \mathcal{K} \pi K_{\max}^4/24 \sigma_f^3 \mu \delta a. \quad (39)$$

Inserting equation (39) into (35) gives for σ_f

$$\sigma_f = (\sigma_0/D_0^m)^{1/(3m+1)} (\mathcal{K} \pi K_{\max}^4/24 \delta a)^{m/(3m+1)} \quad (40)$$

when the term σ_f' is relatively unimportant.

Inserting equation (40) into (37) gives the following equation for the incremental crack growth δa per cycle

$$\delta a = (\mathcal{K} \pi K_{\max}^4/24 \mu) (\sigma_0 \beta \sqrt{w}/K_{ch} D_0^m)^{1/(3m+1)m}. \quad (41)$$

This equation is a fourth power Paris equation. Since the fatigue crack growth is essentially determined by an accumulated displacement criterion, a fourth power is what is to be expected [14]. Since the term $K_{ch} = (4 \mu \gamma/\mathcal{K})^{1/2}$ equation (41) predicts that any environment that reduces the surface energy will increase the crack growth rate.

It should be emphasized that equation (41) is not valid if either K_{\max} is so large that fracture occurs under a monotonic increase of the stress towards the value σ_{\max} . Equation (41) also is not valid if K_{\max} is so small that the friction stress is never reached on the slip planes. If no slip occurs on these planes the crack will not propagate in fatigue. Thus, if $K_{\max}/(2\pi w)^{1/2}$ is smaller than the friction stress, clearly no fatigue crack propagation can take place. In other words, a threshold effect exists.

DISCUSSION

The original impetus for this paper was to see if a difference between the published results of the first and last authors [1, 2] could be resolved. In one of these earlier calculations, the fracture stress calculated for the elastic enclave model was shown to be proportional to $\gamma^{1/2}$ where γ is the surface energy. In the other, the fracture stress contained in a more complex power relation. In further work, one of us [10] has also shown that this discrepancy is due to the way one estimates the ratio of the plastic zone radius to the elastic enclave radius. However, in all calculations of those sorts, in which continuum plasticity is used in a cut-off procedure at the elastic zone boundary, very severe problems are encountered regarding the kind of boundary condition to use at the elastic enclave radius. In this paper, we have thus adopted a relatively self-consistent one dimensional dislocation model where the boundary condition at the "elastic enclave" radius is not a problem.

The investigation reported here shows that for the one dimensional model, the fracture stress σ_F is the complex power law, equation (27)

$$K_I = (K_{ch}^2/w)^{1/(1+m)} \beta.$$

Here, $K_I = \sigma_f \pi a$ is the critical stress intensity factor at fracture, and a is the half length of the crack. (When the Griffith fracture condition determines the value of K_{Ic} , this term is equal to $\sqrt{4\mu_f \gamma}$.) Unfortunately, however, this result is valid only for the one dimensional model, and the full two (and perhaps three) dimensionality of the slip around the crack tip might yield a still different result.

One of the features of this work is the modification of the classical BCS model of one dimensional slip in front of a crack to include an elastic enclave, or dislocation free zone. Our calculation, though independently arrived at, is a limiting form of other work in press by Majumdar and Burns. This important result shows how the crack tip stress intensity factor K_I can be related to the overall stress intensity factor, K , and it allows us to derive a fracture stress in terms of materials parameters for the one dimensional model.

One of the interesting side features of this investigation was the discovery that all continuum theories such as BCS or ours neglects the self-image term of the dislocations in the crack. This self-image term, which is present only in bonafide discrete calculations is important in determining the intrinsic elastic enclave region around the crack tip, which must otherwise be an unknown parameter, w , in the theory. In our work, w is either a scale parameter determined by the crystalline heterogeneity of plastic flaw in the material, or as a lower limit, it is given by the self-image term calculable in a discrete dislocation model.

In our model, we have also demonstrated one of the curiosities of the dislocation shielding theory, namely that under certain conditions it is possible for the shielding to be zero. In particular for a group of dislocations on certain slip planes in equilibrium with a certain kind of friction stress of which $\sigma_f = \text{const.}$ is a special case, and where the total summed burgers vector is zero, the shielding is zero.

Finally, we have applied these ideas to cyclic fatigue. In qualitative terms we showed that when the external stress cycles to "off", the large screening dislocation distribution near the crack tip explodes under the internal pressure of the mutual repulsive forces between the dislocations. Many of the dislocations are pushed behind the crack, and "annihilated" there by the images in the crack faces, and the remainder left in front of the crack is that total number which can establish a new equilibrium in the

distance R under the slip plane friction stress, $\sigma_f(x)$. This residual shielding distribution provides a closure stress on the tip which may drive the crack tip backwards, and in any case will weld portions of the cleavage plane back together.

When the external stress is switched back "on" the K -field of the crack regenerates the shielding charge partly by action sources on the slip plane, and partly by moving the "annihilated" dislocations back into a shielding configuration in front of the crack.

If there is no work hardening, the dislocation distribution is essentially reversible under the stress: i.e. the sources can regenerate exactly the same distribution as in the previous cycle, with the crack in an unchanged position. However if there is strain hardening, the sources are unable, at the same stress, to regenerate the same shielding charge; K_I rises above K_{Ic} , and the crack moves forward to a position where fresh sources can be activated. Thus in our view, fatigue growth of the crack is due to strain hardening during stress cycling. Quantitative analysis indicates that a fourth power Paris equation describes the crack growth law.

Acknowledgement The research of one of us (J.W.) was supported by the National Science Foundation, through the Materials Research Center of the Northwestern University, under grant No. DMR 7601057.

REFERENCES

1. R. Thompson, *J. Mater. Sci.* **13**, 128 (1978).
2. J. Weertman, *Acta metall.* **26**, 1731 (1978).
3. B. A. Bilby, A. H. Cottrell and K. H. Swinden, *Proc. R. Soc.* **272**, 304 (1963).
4. R. Thomson and J. Sinclair, *Acta metall.* **30**, 1325 (1982).
5. J. Rice, *J. appl. Mech.* **35**, 379 (1968).
6. J. D. Eshelby, *Phil. Trans. R. Soc.* **A244**, 87 (1951).
7. N. I. Muskhelishvili, *Some Basic Problems of the Mathematical Theory of Elasticity*, pp. 253-282. Noordhoff, Groningen (1953).
8. J. Rice and R. Thomson, *Phil. Mag.* **29**, 73 (1974).
9. N. I. Muskhelishvili, *Singular Integral Equations*. Noordhoff, Groningen (1953).
10. A. H. Head and N. Louat, *Aust. J. Phys.* **8**, 1 (1955).
11. S. J. Chang and S. M. Ohr, *J. appl. Phys.* **52**, 7174 (1981).
12. B. S. Majumdar and S. J. Burns, *Int. J. Fract. Mech.* To be published.
13. R. Thomson and E. Fuller, in *Micro and Macro Mechanics of Crack Growth* (edited by K. Sadananda, B. B. Rath and D. J. Michel), pp. 49-59. Met Soc. A.I.M.E.
14. J. Weertman, in *Fatigue and Microstructure*, pp. 279-306. Am. Soc. Metals, Metals Park, OH (1979).

Accession For		Distribution/		Availability Codes	
NTIS GRA&I	<input checked="" type="checkbox"/>			Avail end/or	Special
DTIC TAB	<input type="checkbox"/>			Dist	A 21
Unannounced	<input type="checkbox"/>				
Justification					